(This is a sample cover image for this issue. The actual cover is not yet available at this time.)

Mechanics Research Communications 47 (2013) 44–49

Contents lists available at SciVerse ScienceDirect

Mechanics Research Communications

journal homepage: www.elsevier.com/locate/mechrescom

The influence of the shear deformations on the local stress state of pultruded composite profiles

Luciano Feo, Geminiano Mancusi*

Department of Civil Engineering, University of Salerno, 84084 Fisciano, Italy

ARTICLE INFO

Article history:
Received 12 September 2012
Received in revised form 6 November 2012
Available online xxx

Keywords:
Thin-walled beams
Composites
Shear deformability
Finite element analysis

ABSTRACT

Due to the relevance of shear deformability, the practical use of composite profiles still conflicts with the serviceability requirements related to the stiffness demand for civil applications. Moreover, when dealing with shear deformable beams, it is also well recognized that displacement-based 1-D models can lead to inaccurate stress predictions.

Hence, a relatively simple beam model allowing to evaluate both strains and stresses accurately may represent a useful tool.

The main motivation of the present paper is precisely to investigate these features by presenting relevant numerical results dealing with the mechanical response of pultruded composite profiles with thin-walled open cross-section made of both Glass (GFRP) and Carbon Fiber Reinforced Plastic (CFRP).

Comparisons with solutions given via classical 1-D/2-D mechanical models are also provided, which highlight the accuracy of the proposed kinematics, especially with the aim of a reliable stress evaluation.

1. Introduction

Fiber-reinforced composite materials (FRP), already extensively studied by many authors (Barbero, 1993; Massa and Barbero, 1998; Mudder and Chaturvedi, 1999; Vasiliev and Jones, 1993; Winson and Sierakowski, 1987), are spreading in the field of civil engineering and, in particular, in the field of structural rehabilitation.

In this context, FRPs have been used successfully for a decade ago for the retrofitting of structural elements made of masonry (Ascione et al., 2005a), reinforced concrete (Ascione et al., 2005b; Mancusi et al., 2012a), steel and wood.

Although many international codes or guide-lines provide specific rules concerning the strengthening of pre-existing members, which are thereby helpful in the design of such interventions and, at the same time, have encouraged their use, more effort has still to be made in order to investigate the use of FRP profiles for constructions entirely made of FRP, necessarily accounting for the shear deformability (Feo and Mancusi, 2010; Minghini et al., 2007), which obviously affects the buckling behavior (Minghini et al., 2008, 2009a,b; Mancusi and Feo, 2012), the dynamic behavior (Minghini et al., 2010), the long term behavior, i.e. creep (Ascione et al., 2012; Mancusi et al., 2012b), the joint behavior (Ascione and Mancusi, 2010a,b).

This paper aims at contributing to the evaluation of the reliability of constructions entirely made of pultruded composite profiles, that are becoming increasingly numerous, especially in some specific contexts such as bridge decks, large span roofs and footbridges, where the main advantages of pultruded composite profiles clearly emerge: lightness; high strength to weight and stiffness to weight ratios; resistance against corrosion.

A correct use of the pultruded composites requires, in fact, an accurate assessment of both short and long term stresses and strains. In particular, the mechanical behavior of FRP profiles depends on numerous factors, such as:

- the shear deformability, no longer negligible due to the rather small values of shear moduli of elasticity;
- the amount of creep strains, potentially detrimental in terms of structural integrity and/or serviceability performance;
- the brittle connotation of failure mechanisms, which requires an accurate stress prediction.

In the present work a finite element numerical investigation on the short-term static behavior of FRP pultruded elements is presented. The main aim is to investigate the influence of the shear deformations on the prediction of the stress state.

The simulations are based on a one-dimensional mechanical model previously presented by the authors which is specifically formulated to analyze the effects of the shear deformations (Ascione et al., 2000; Feo and Mancusi, 2010). The numerical results are

* Corresponding author.
E-mail addresses: l.feo@unisa.it (L. Feo), g.mancusi@unisa.it (G. Mancusi).

0093-6413/$ – see front matter © 2012 Elsevier Ltd. All rights reserved.
http://dx.doi.org/10.1016/j.mechrescom.2012.11.004

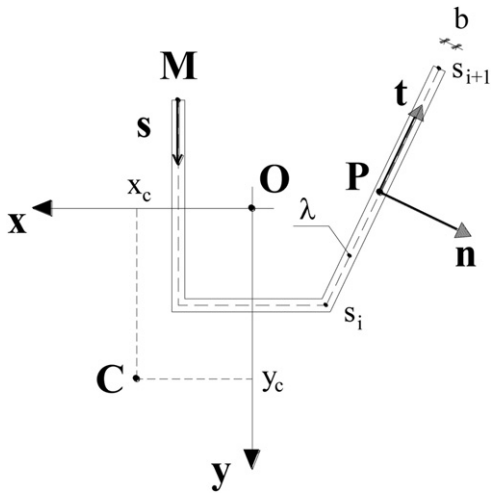

Fig. 1. Cross-section of a thin-walled beam.

compared with those obtained via both classical Timoshenko and Vlasov models, or via finite element analyses in 2-D elasticity under plane stress hypothesis.

2. Kinematic model

The kinematics of a thin-walled beam, as discussed elsewhere (Feo and Mancusi, 2010), has been modeled as follows (Fig. 1):

$$\xi = \xi(s,z) = \xi_c(z) - \rho(z)\cdot(y(s) - y_c), \tag{1a}$$

$$\eta = \eta(s,z) = \eta_c(z) + \rho(z)\cdot(x(s) - x_c), \tag{1b}$$

$$\zeta = \zeta(s,z) = \zeta_c(z) - \beta(z)\cdot x(s) + \alpha(z)\cdot y(s) - \rho'(z)\cdot\omega(z) + \gamma_i(z)\cdot\omega_i(s). \tag{1c}$$

In Eq. (1a)–(1c) x_c, y_c correspond to the coordinates of a fixed point C assumed as pole of a rigid transformation; $\xi_c(z)$, $\eta_c(z)$ are the displacement components of the point C along the x and y axes, respectively; $\alpha(z)$ and $\beta(z)$ are the cross-section flexural rotations. Furthermore, the following position exists: $\zeta_c(z) = \zeta_M(z) + \beta(z)\cdot x_M - \alpha(z)\cdot y_M$ with $\zeta_M = \zeta|_{s=0}$ and $M(x_M, y_M)$ denoting the origin of the curvilinear abscissa s. Moreover, $\rho'(z)$ is the derivative of the twisting rotation $\rho(z)$ with respect to the z coordinate while $\omega(s)$ is the current sectorial area as in the classical theory of thin-walled beams (Vlasov, 1961). Finally, the terms $\gamma_i(z)$ ($i = 1, 2, \ldots, N_s$) are further generalized kinematical unknowns conjugated with the geometrical quantities $\omega_i(z)$, defined as:

$$\omega_i(s) = \int_M^P f_i(t)dt, \tag{2}$$

In Eq. (2) the symbol f_i denotes a polynomial of the curvilinear coordinate.

The authors stress the importance for the reader to consult a previous theoretical paper (Feo and Mancusi, 2010), which concerns the extended formulation of the beam model. Here they just limit the discussion remarking that the additional terms $\gamma_i(z)$provide a more refined modeling of shear deformability as the parameter N_s increases.

Finally, it is possible to recognize that the displacement field components (1a)–(1c) allow the generic cross-section depicted in Fig. 1 to exhibit: (i) a rigid transformation in its own plane; (ii) a warping out of the same plane; and (iii) the following angular sliding along the mid-line λ:

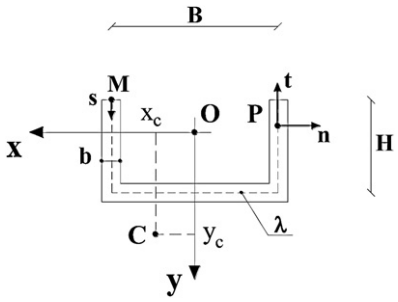

Fig. 2. Cross-section under consideration.

$$\gamma_{tz}(n,s,z)\big|_{n=0} = \gamma_{xz}^{(0)}(z)\frac{dx}{ds} + \gamma_{yz}^{(0)}(z)\frac{dy}{ds} + \gamma_i(z)f_i(s), \tag{3}$$

A few comments are appropriate.

The expression for the longitudinal displacement given by Eq. (1c) may lead to serious difficulties in modeling the continuity conditions between contiguous beams with the axes being non-parallel. The high accuracy of the model, in fact, is obtained by increasing the number N_s of the additional warping functions and this unavoidably yields a high numerical complexity even in the case of typical portal frames. This point still requires a further investigation.

The relevance of shear strains, which are absent in the classical theory of Vlasov, it is clearly understandable taking into account the small values of the shear moduli exhibited by pultruded composite beams, which are substantially coincident with those of the resin. Their influence can be captured by the proposed 1-D model with the same accuracy of more complex 2-D finite element models (being this the actual goal of the authors) only if the number of additional warping functions is appropriate. This number is related to a parameter (N_o) denoting the maximum polynomial exponent, as discussed in Feo and Mancusi (2010), where many simulations obtained for different values of No are compared.

Given that polynomials up to the third order are found able to guarantee the best accuracy in terms of predicted stresses, deflections and rotations, the required number of additional warping functions generally depends on the geometry of the cross-section. According to the multi-step procedure proposed in Feo and Mancusi (2010) for cross-sections made of interconnected thin rectangles, it results $N_s = (N_o + 1)\times N_{seg} - 2$, where N_{seg} denotes the number of rectangles.

Hence, $N_o = 3$ implies $N_s = 10$ if $N_{seg} = 3$, as for the shape considered in Section 3.

As expected, when the additional kinematic variables $\gamma_i(z)$ are constrained, a loss of accuracy is found in the neighborhood of the corresponding cross-section. This error mainly affects the prediction of the internal stresses close to the considered cross-section, but it suddenly vanishes. A theoretical estimation of the distance from singularities at which the proposed model begins to lose accuracy still requires a further investigation.

3. Numerical analyses

Numerical analyses have covered the static behavior of pultruded "U" profiles (dimensions $360\times108\times18$) made of CFRP or GFRP. With reference to the symbols indicated in Fig. 2, the following assumptions have been made: $B = 342$ mm, $H = 99$ mm, $b = 18$ mm, coinciding with the cross-section dimensions of a GFRP U-profile manufactured by Fiberline Composites (FC).

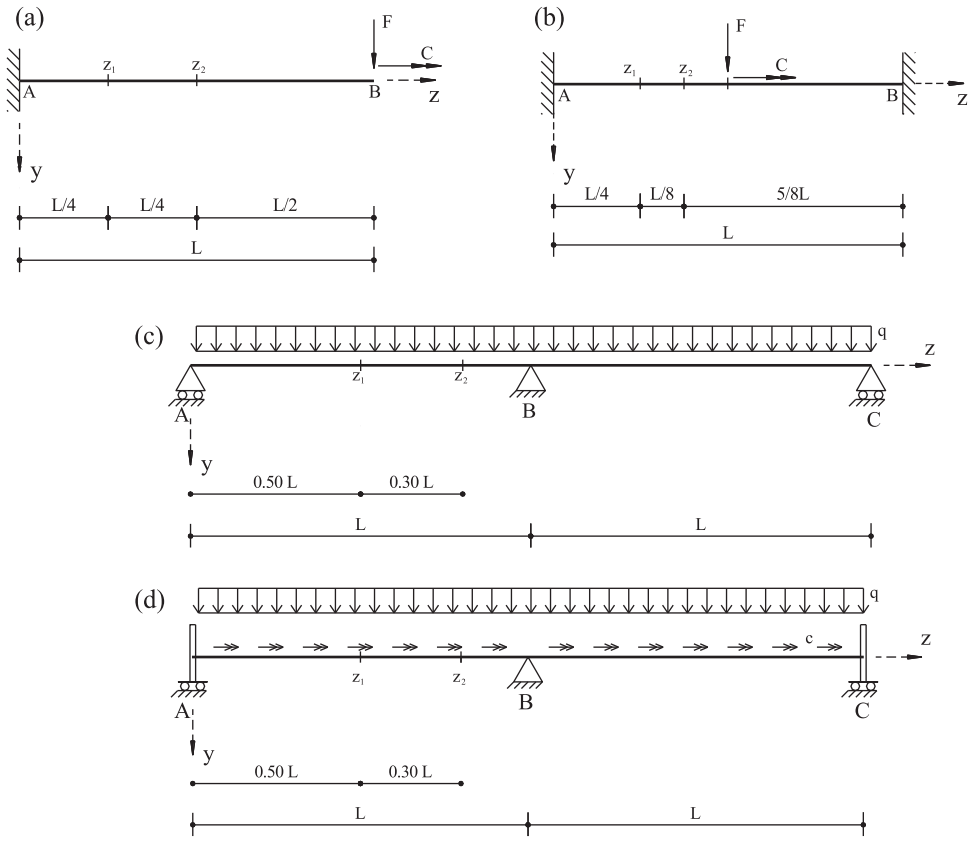

Fig. 3. (a) Scheme 1. Cantilever beam ($F = 1$ N – $C = 0.171$ N m) (b) Scheme 2. Hyper static beam ($F = 1$ N – $C = 0.171$ N m). (c) Scheme 3. Two-span beam ($q = 1$ N/m). (d) Scheme 4. Two-span beam ($q = 1$ N/m; $c = 0.171$ N m/m).

The proposed 1-D model incorporates a simple linear elastic (up to failure) constitutive law which requires only two elastic moduli to be determined:

$$\begin{bmatrix} \tau_{tz} \\ \sigma_{zz} \end{bmatrix} = \begin{bmatrix} G_{tz} & 0 \\ 0 & D_{zz} \end{bmatrix} \begin{bmatrix} \gamma_{tz} \\ \varepsilon_{zz} \end{bmatrix} \tag{4}$$

being D_{zz} the longitudinal normal modulus ($D_{zz} = E_L$) while G_{tz} the shear modulus relative to the directions **t** and **k** ($G_{tz} = G_{TL}$). Due to the considered orientation of the fibers, which are aligned to the **k** unit vector (i.e. the pultrusion axis), the out of diagonal terms in Eq. (4) are not present.

For the purpose of completeness, all elastic moduli have been listed in Tables 1 and 2. They concern typical epoxy resin FRP profiles. Table 1 refers to carbon fiber-composite profiles (CFRP), while Table 2 refers to glass fiber-composite profiles (GFRP). Transverse isotropy has been accounted for.

In the previous Tables 1 and 2, the subscripts N, T and L denote the natural system $\{N, T, L\}$ in which L corresponds to the fiber orientation (longitudinal axis of the beam), and N and T correspond to the axes n and t (Fig. 1), respectively.

In addition to $\boldsymbol{E_L}$ and $\boldsymbol{G_{TL}}$, which are required for the constitutive law given in Eq. (4), other moduli will be utilized for 2-D elastic analyses, as stated in the following.

The structural schemes examined are illustrated in Fig. 3a–d.

While the Scheme 1deals with a cantilever beam under a shear force and a torsion couple applied at the free end, the other schemes, which instead are hyperstatic, refer to: a beam with rotationally fixed supports under a shear force and a torsional couple applied at mid-span cross-section (Scheme 2); a two-spam beam under a transverse uniform load per unit length (Scheme 3); a two-spam beam under a transverse uniform load and torsional couple per unit length with supports preventing torsional rotations but allowing both flexural rotations and warping (Scheme 4).

The length parameter L assumes the following values: $L = 3.0$ m, $L = 5.0$ m.

The beam axis has been discretized by a uniform mesh consisting of "Hermitian" finite elements; due to evident symmetry, the discretization of two-span beams (Schemes 3 and 4) has concerned one span only. A uniform mesh consisting of sixty finite elements has been employed. More details are given in Feo and Mancusi (2010).

For what concern the numerical simulations presented, the polynomials f_i have been considered up to the third order. As previously remarked, this ensures the best approximation of the numerical prediction with respect to the solutions given via 2-D elastic analyses.

Table 1
Elastic moduli – CFRP.

Young moduli (MPa)	$E_N = 8800$	$E_T = 8800$	$E_L = 115{,}000$
Poisson moduli	$\nu_{NT} = 0.5720$	$\nu_{NL} = 0.2168$	$\nu_{TL} = 0.2168$
Shear moduli (MPa)	$G_{NT} = 2800$	$G_{NL} = 3100$	$G_{TL} = 3100$

Table 2
Elastic moduli – GFRP.

Young moduli (MPa)	$E_N = 8500$	$E_T = 8500$	$E_L = 23{,}000$
Poisson moduli	$\nu_{NT} = 0.42$	$\nu_{NL} = 0.09$	$\nu_{TL} = 0.09$
Shear moduli (MPa)	$G_{NT} = 3000$	$G_{NL} = 3000$	$G_{TL} = 3000$

Table 3
Convergence test.

Scheme	L (m)	Generalized displacement under monitoring	Monitored values					
			Number of finite element employed over a single span					
			2	4	10	50	60	70
1	3.0	Deflection (end B) (m)	9.82218×10^{-6}	9.82369×10^{-6}	9.82411×10^{-6}	9.82415×10^{-6}	9.82415×10^{-6}	9.82415×10^{-6}
	5.0		4.38587×10^{-5}	4.38627×10^{-5}	4.38639×10^{-5}	4.38641×10^{-5}	4.38641×10^{-5}	4.38641×10^{-5}
2	3.0	Mid-span deflection (m)	2.52001×10^{-7}	2.55730×10^{-7}	2.58593×10^{-7}	2.59977×10^{-7}	2.60060×10^{-7}	2.60060×10^{-7}
	5.0		8.67559×10^{-7}	8.74397×10^{-7}	8.79604×10^{-7}	8.82165×10^{-7}	8.82210×10^{-7}	8.82210×10^{-7}
3	3.0	Flexural rotation (end A)	-7.52103×10^{-7}	-7.48244×10^{-7}	-7.47739×10^{-7}	-7.47720×10^{-7}	-7.47720×10^{-7}	-7.47720×10^{-7}
	5.0		-3.02537×10^{-6}	-3.00383×10^{-6}	-3.00103×10^{-6}	-3.00090×10^{-6}	-3.00090×10^{-6}	-3.00090×10^{-6}
4	3.0	Torsional rotation (support B)	9.03321×10^{-5}	9.03090×10^{-5}	9.03073×10^{-5}	9.03072×10^{-5}	9.03072×10^{-5}	9.03072×10^{-5}
	5.0		4.15723×10^{-4}	4.15632×10^{-4}	4.15625×10^{-4}	4.15625×10^{-4}	4.15625×10^{-4}	4.15625×10^{-4}

3.1. Convergence

The Table 3 presents many tests developed by the authors in order to assess the convergence rate of the numerical model proposed. The tests are limited to the analysis of CFRP beams only. A mesh composed of at least ten finite elements seems to exhibit a sufficient accuracy.

3.2. Numerical results

The Table 4a–d propose many numerical results obtained via the present theory (P.T.). They are compared with the results predicted by using the Vlasov kinematics (VL), which preserves any generic cross-section un-deformed in its own plane, allows the cross section to warp but does not allow the mid-line λ to exhibit shear strains. Percentage differences are also presented with reference to the Vlasov solution.

In Figs. 4a, b and 5a, b comparisons are given in terms of tangential and normal stresses (unit MPa) along the mid-line λ evaluated by using the present theory (P.T.), the Vlasov theory (VL) and, last, a 2-D finite element analysis performed by means of a standard code (ST.) (Straus 7). In particular, the *mesh* adopted for 2-D analyses subdivides the mid-plane of the thin-walled beam by 20 elements (along the mid-line λ) $\times$ 30 or 50 elements (along the longitudinal axis), the last choice depending on the value of the length $L = 3.0$ m or $L = 5.0$ m, respectively. The comparisons are limited to the CFRP beams of Schemes 1 and 2 with a length $L = 5.0$ m.

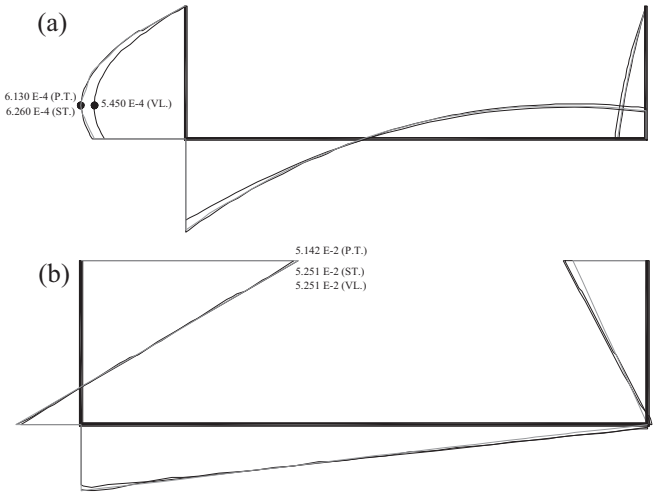

Fig. 4. (a) Tangential stresses along the mid-line λ. (Scheme 1 – $L = 5.0$ m, $z = 1/4\,L$ – CFRP). (b) Normal stresses along the mid-line λ. (Scheme 1 – $L = 5.0$ m, $z = 1/4\,L$ – CFRP).

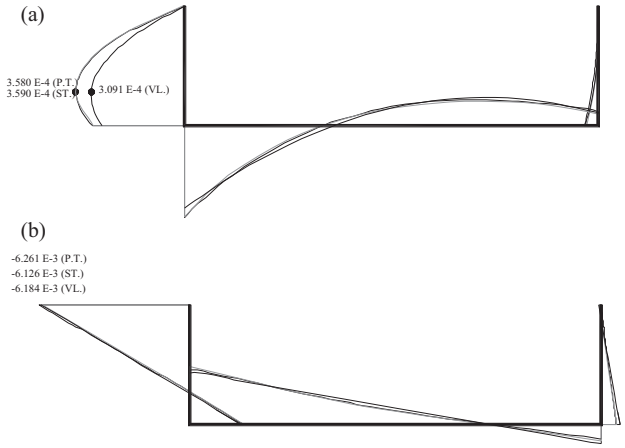

Fig. 5. (a) Tangential stresses along the mid-line λ. (Scheme 2 – $L = 5.0$ m, $z = 3/8\,L$ – CFRP). (b) Normal stresses along the mid-line λ. (Scheme 2 – $L = 5.0$ m, $z = 3/8\,L$ – CFRP).

Furthermore, Figs. 6a, b and 7a and b allow to compare tangential and normal stresses evaluated by the proposed model (P.T.) with reference to both CFRP and GFRP beams. The comparisons are limited to Schemes 3 and 4, which are hyper static, and refer to the length $L = 3.0$ m. A not negligible dependence on the elastic moduli has been found.

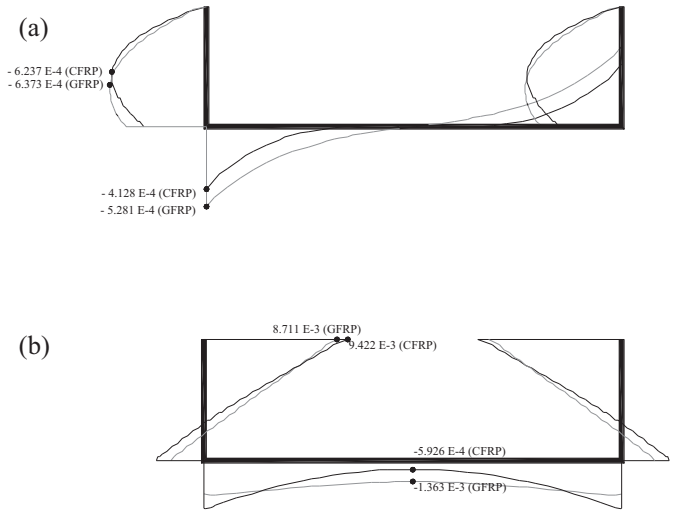

Fig. 6. (a) Tangential stresses along the mid-line λ (P.T.) Comparison between CFRP and GFRP beams (Scheme 3 – $L = 3.0$ m, $z = L$). (b) Normal stresses along the mid-line λ (P.T.) Comparison between CFRP and GFRP beams (Scheme 3 – $L = 3.0$ m, $z = L$).

Table 4
Comparisons – Schemes 1 (a), Schemes 2 (b), Schemes 3 (c), Schemes 4 (d).

(a)

Length (m)	Material	Displacement/rotation (end B)	P.T.	VL	Var. (%)
3.0	CFRP	Deflection (m)	9.824×10^{-6}	9.271×10^{-6}	5.63
5.0			4.386×10^{-5}	4.292×10^{-5}	2.14
3.0		Flexural rotation	-4.740×10^{-6}	-4.635×10^{-6}	2.22
5.0			-1.299×10^{-5}	-1.288×10^{-5}	0.85
3.0		Torsional rotation	4.900×10^{-5}	4.786×10^{-5}	2.33
5.0			1.366×10^{-4}	1.356×10^{-4}	0.73
3.0	GFRP	Deflection (m)	4.694×10^{-5}	4.635×10^{-5}	1.26
5.0			2.155×10^{-4}	2.146×10^{-4}	0.42
3.0		Flexural rotation	-2.328×10^{-5}	-2.318×10^{-5}	0.43
5.0			-6.448×10^{-5}	-6.438×10^{-5}	0.16
3.0		Torsional rotation	1.020×10^{-4}	1.016×10^{-4}	0.39
5.0			2.099×10^{-4}	2.095×10^{-4}	0.19

(b)

Length (m)	Material	Displacement/rotation (mid-span)	P.T.	VL	Var. (%)
3.0	CFRP	Deflection (m)	2.601×10^{-7}	1.449×10^{-7}	44.29
5.0			8.822×10^{-7}	6.706×10^{-7}	23.99
3.0		Torsional rotation	1.635×10^{-6}	1.132×10^{-6}	30.76
5.0			5.726×10^{-6}	4.937×10^{-6}	13.78
3.0	GFRP	Deflection (m)	8.600×10^{-7}	7.423×10^{-7}	13.69
5.0			3.589×10^{-6}	3.353×10^{-6}	6.58
3.0		Torsional rotation	5.443×10^{-6}	4.999×10^{-6}	8.16
5.0			1.889×10^{-5}	1.837×10^{-5}	2.75

(c)

Length (m)	Material	Displacement/rotation	P.T.	VL	Var. (%)
3.0	CFRP	Deflection (m) ($z = 0.50 \cdot L$)	6.501×10^{-7}	4.345×10^{-7}	33.16
5.0			4.003×10^{-6}	3.353×10^{-6}	16.24
3.0		Flexural rotation (support A)	-7.477×10^{-7}	-5.794×10^{-7}	22.51
5.0			-3.001×10^{-6}	-2.683×10^{-6}	10.60
3.0	GFRP	Deflection (m) ($z = 0.50 \cdot L$)	2.422×10^{-6}	2.173×10^{-6}	10.28
5.0			1.748×10^{-5}	1.677×10^{-5}	4.06
3.0		Flexural rotation (support A)	-3.103×10^{-6}	-2.897×10^{-6}	6.64
5.0			-1.378×10^{-5}	-1.341×10^{-5}	2.69

(d)

Length (m)	Material	Displacement/rotation	P.T.	VL	Var. (%)
3.0	CFRP	Deflection (m) ($z = 0.50 \cdot L$)	6.501×10^{-7}	4.345×10^{-7}	33.16
5.0			4.003×10^{-6}	3.353×10^{-6}	16.24
3.0		Flexural rotation (support A)	-7.477×10^{-7}	-5.794×10^{-7}	22.51
5.0			-3.001×10^{-6}	-2.683×10^{-6}	10.60
3.0		Torsional rotation (support B)	9.031×10^{-5}	8.893×10^{-5}	1.53
5.0			4.156×10^{-4}	4.144×10^{-4}	0.29
3.0	GFRP	Deflection (m) ($z = 0.50 \cdot L$)	2.422×10^{-6}	2.173×10^{-6}	10.28
5.0			1.748×10^{-5}	1.677×10^{-5}	4.06
3.0		Flexural rotation (support A)	-3.103×10^{-6}	-2.897×10^{-6}	6.64
5.0			-1.378×10^{-5}	-1.341×10^{-5}	2.69
3.0		Torsional rotation (support B)	1.840×10^{-4}	1.838×10^{-4}	0.11
5.0			6.098×10^{-4}	6.097×10^{-4}	0.02

Table 5
Comparisons in terms of deflections and rotations.

Scheme	L (m)	Generalized displacement	CFRP			GFRP		
			P.T.	VL	TM	P.T.	VL	TM
1	3.0	Deflection (end B) (m)	9.824×10^{-6}	9.271×10^{-6}	9.856×10^{-6}	4.694×10^{-5}	4.635×10^{-5}	4.696×10^{-5}
	5.0		4.386×10^{-5}	4.292×10^{-5}	4.390×10^{-5}	2.155×10^{-4}	2.146×10^{-4}	2.156×10^{-4}
2	3.0	Mid-span deflection (m)	2.601×10^{-7}	1.449×10^{-7}	2.912×10^{-7}	8.600×10^{-7}	7.423×10^{-7}	8.755×10^{-6}
	5.0		8.822×10^{-7}	6.706×10^{-7}	9.145×10^{-7}	3.589×10^{-6}	3.353×10^{-6}	3.605×10^{-6}
3	3.0	Flexural rotation (end A)	-7.477×10^{-7}	-5.794×10^{-7}	-6.827×10^{-7}	-3.103×10^{-6}	-2.897×10^{-6}	-3.009×10^{-6}
	5.0		-3.001×10^{-6}	-2.683×10^{-6}	-2.861×10^{-6}	-1.378×10^{-5}	-1.341×10^{-5}	-1.360×10^{-5}
4	3.0	Torsional rotation (support B)	9.031×10^{-5}	8.893×10^{-5}	–	1.840×10^{-4}	1.838×10^{-4}	–
	5.0		4.156×10^{-4}	4.144×10^{-4}	–	6.098×10^{-4}	6.097×10^{-4}	–

Table 6
Comparisons in terms of deflections and rotations (percentage differences).

Scheme	L (m)	Generalized displacement	CFRP		GFRP	
			Var. 1 (%)	Var. 2 (%)	Var. 1 (%)	Var. 2 (%)
1	3.0	Deflection (end B) (m)	5.96	−0.32	1.27	−0.04
	5.0		2.19	−0.09	0.42	−0.05
2	3.0	Mid-span deflection	79.50	−10.68	15.86	−1.77
	5.0	(m)	31.55	−3.53	7.04	−0.44
3	3.0	Flexural rotation (end	29.05	9.52	7.11	3.12
	5.0	A)	11.85	4.89	2.76	1.32
4	3.0	Torsional rotation	1.55	–	0.11	–
	5.0	(support B)	0.29	–	0.02	–

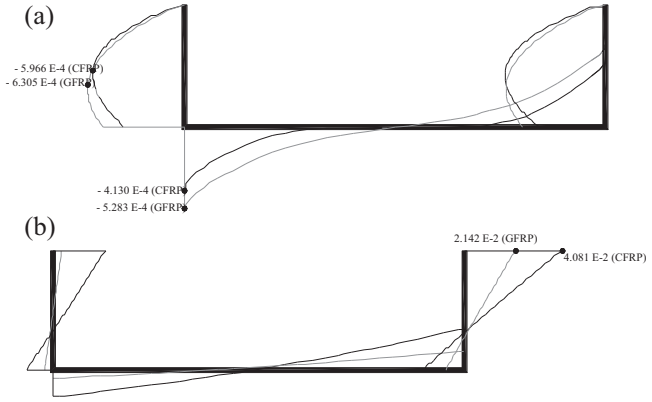

Fig. 7. (a) Tangential stresses along the mid-line λ (P.T.) Comparison between CFRP and GFRP beams (Scheme 4 – $L = 3.0$ m, $z = L$). (b) Normal stresses along the mid-line λ (P.T.) Comparison between CFRP and GFRP beams (Scheme 4 – $L = 3.0$ m, $z = L$).

Finally, in Table 5, displacements and flexural/torsional rotations are compared with those given via the Vlasov (VL) and the Timoshenko (T.M.) beam models. In the last case the evaluations have been made assuming the following shear corrective factor: $\chi = 5.88$.

The corresponding percentage differences with reference to both the Vlasov beam solution (Var. 1) and the Timoshenko beam solution (Var. 2) are also presented in Table 6.

4. Conclusions

The simulations presented show the accuracy of the mechanical model proposed by the authors for the study of the static behavior of pultruded composite profiles. Comparisons in terms of stress components show a substantial agreement between the values predicted by the authors and those evaluated via a two-dimensional mechanical modeling. More or less marked differences were found, however, in comparison with the classical theory of sectorial areas.In fact, for the beams considered, differences of about 16% and 2% were found with regard to shear and normal stresses, respectively. Moreover, for the CFRP beams, the deflections and the flexural rotations predicted by the proposed model are about 80% (Schemes 2 with $L = 3.0$ m) and 29% (Schemes 3 with $L = 3.0$ m) greater, respectively. For the GFRP beams the influence of the shear deformation decreases and the percentage differences with respect to Vlasov's theory become +16% and +7% for deflections and flexural rotations, respectively. Comparison, however, with the predictions obtained via the Timoshenko beam model indicate differences in terms of displacement up to −11% (Scheme 2 with $L = 3.0$ m – CFRP) and, in terms of rotation, up to +10% (Scheme 3 with $L = 3.0$ m – CFRP). Furthermore, for cases relating to the GFRP material, the difference between the proposed model and the solution of Timoshenko beam is quite negligible.

It emerges that the proposed model, although belonging to the group of one-dimensional models, is able to capture displacements and stresses with high accuracy. This property is particularly important in view of the brittle nature of the FRP composites, since an accurate stress evaluation is at the base of a correct use of any failure criteria.

References

Ascione, L., Feo, L., Mancusi, G., 2000. On the statical behaviour of FRP thin walled beams. Composites Part B: Engineering 31 (8), 643–654.

Ascione, L., Feo, L., Fraternali, F., 2005a. Load carrying capacity of 2D FRP/strengthened masonry structures. Composites Part B: Engineering 36 (8), 619–626.

Ascione, L., Berardi, V.P., Feo, L., Mancusi, G., 2005b. A numerical evaluation of the interlaminar stress state in externally FRP plated RC beams. Composites Part B: Engineering 36 (1), 83–90.

Ascione, L., Berardi, V.P., D'Aponte, A., 2012. Creep phenomena in FRP materials. Mechanics Research Communications 43, 15–21.

Ascione, F., Mancusi, G., 2010a. Axial/bending coupled analysis for FRP adhesive lap joints. Mechanics of Advanced Materials and Structures 17 (2), 85–98.

Ascione, F., Mancusi, G., 2010b. Failure criteria for FRP adhesive lap joints: a comparative analysis. Mechanics of Advanced Materials and Structures 17 (2), 157–164.

Barbero, E.J., 1993. Introduction to Composite Material Design. Taylor & Francis, Bristol, PA.

Feo, L., Mancusi, G., 2010. Modeling shear deformability of thin-walled composite beams with open cross-section. Mechanics Research Communications 37 (3), 320–325.

FC. Fiberline Composites – http://www.fiberline.com

Mancusi, G., Feo, L., Berardi, V.P., 2012a. Concrete open-wall systems wrapped with FRP under torsional loads. Materials 11, 2055–2068.

Mancusi, G., Spadea, S., Berardi, V.P., 2012b. Experimental analysis on the time-dependent bonding of FRP laminates under sustained loads. Composites Part B: Engineering, http://dx.doi.org/10.1016/j.compositesb.2012.10.007.

Mancusi, G., Feo, L.,2012. Non-linear pre-buckling behavior of shear deformable thin-walled composite beams with open cross-section. Composites Part B, http://dx.doi.org/10.1016/j.compositesb.2012.11.003, in press.

Massa, J.C., Barbero, E.J., 1998. A strength of materials formulation for thin walled composite beams with torsion. Journal of Composite Materials, 1560–1594.

Minghini, F., Tullini, N., Laudiero, F., 2007. Locking-free finite elements for shear deformable orthotropic thin-walled beams. Int. J. Numer. Meth. Eng. 72, 808–834.

Minghini, F., Tullini, N., Laudiero, F., 2008. Buckling analysis of FRP pultruded frames using locking-free finite elements. Thin-Walled Structures 46, 223–241.

Minghini, F., Tullini, N., Laudiero, F., 2009a. Vibration analysis with second-order effects of pultruded FRP frames using locking-free elements. Thin-Walled Structures, 136–150.

Minghini, F., Tullini, N., Laudiero, F., 2009b. Elastic buckling analysis of pultruded FRP portal frames having semi-rigid connections. Eng. Struct. 31, 292–299.

Minghini, F., Tullini, N., Laudiero, F., 2010. Vibration analysis of pultruded FRP frames with semi-rigid connections. Eng. Struct. 32, 3344–3354.

Mudder, S.S., Chaturvedi, S.K., 1999. Laminated composite open profile sections: first order shear deformation theory. Composite Structures, 105–114.

STRAUS 7, 2004. Theoretical Manual – Theoretical Background to the Straus7 Finite Element Analysis System.

Vasiliev, V.V., Jones, R.M. (Eds.), 1993. Mechanics of Composite Structures. Taylor & Francis.

Vlasov, V.Z., 1961. Thin-Walled Elastic Beams. Pergamon Press, New York.

Winson, J.R., Sierakowski, R.L., 1987. The Behaviour of Structures Composed of Composite Materials. Nijhoff Publishers, Dordrecht.